(2)

FLUCTUATION ANALYSIS OF LIQUID/LIQUID AND GEL/LIQUID INTERFACES

Vladimír Mareček

The J.Heyrovský Institute of Physical Chemistry and Electrochemistry,

Dolejskova 3, 182 23 Prague 8, Czechoslovakia

and

Miklós Gratzl, András Pungor and Jiří Janata

Center for Sensor Technology, University of Utah, Salt Lake City,

Utah 84112, U.S.A.

OFFICE OF NAVAL RESEARCH

Contract NOOO14-87-K-0060

Task No. NR 051-77815-79-81 (472)

TECHNICAL REPORT NO. 17

FLUCTUATION ANALYSIS OF LIQUID/LIQUID AND LIQUID/LIQUID/GEL INTERFACE

by

V.Marecek, M.Gratzl, A.Pungor and J.Janata

Department of Materials Science, University of Utah
Salt Lake City, Utah 84112

Accepted for publication in Journal of Electroanalytical and Interfacial Chemistry
1989

SECURITY CLASSIFICATION OF THIS PAGE

REPORT DOCUMENTATION PAGE

1a. REPORT SECURITY CLASSIFICATION	1b. RESTRICTIVE MARKINGS
2a. SECURITY CLASSIFICATION AUTHORITY	3. DISTRIBUTION/AVAILABILITY OF REPORT
2b. DECLASSIFICATION/DOWNGRADING SCHEDULE	Approved for public release, distribution unlimited
4. PERFORMING ORGANIZATION REPORT NUMBER(S)	5. MONITORING ORGANIZATION REPORT NUMBER(S)
Technical Report #17	
6a. NAME OF PERFORMING ORGANIZATION: Materials Science & Eng. Dept. University of Utah; 6b. OFFICE SYMBOL (If applicable)	7a. NAME OF MONITORING ORGANIZATION: Robert Silverman, ONR Resident Representative
6c. ADDRESS (City, State, and ZIP Code): Salt Lake City, UT 84112	7b. ADDRESS (City, State, and ZIP Code): 315 University District Bldg. 1107 N.E. 45th St. Seattle, WA 98105-4631
8a. NAME OF FUNDING/SPONSORING ORGANIZATION: ONR; 8b. OFFICE SYMBOL (If applicable)	9. PROCUREMENT INSTRUMENT IDENTIFICATION NUMBER: N00014-87-K-0060
8c. ADDRESS (City, State, and ZIP Code): Office of Naval Research, Arlington, VA 22217-5000	10. SOURCE OF FUNDING NUMBERS

PROGRAM ELEMENT NO.	PROJECT NO.	TASK NO.	WORK UNIT ACCESSION NO.
NR 051	77815	79	81(427)

11. TITLE (Include Security Classification)
Fluctuation Analysis of Liquid/Liquid and Liquid/Gel Interfaces

12. PERSONAL AUTHOR(S)
V. Maracek, M. Gratzl, A. Pungor and J. Janata

13a. TYPE OF REPORT	13b. TIME COVERED	14. DATE OF REPORT (Year, Month, Day)	15. PAGE COUNT
Interim	FROM _____ TO _____	17 March 1989	

16. SUPPLEMENTARY NOTATION
Accepted for publication in J. Electroanal. Chem.

17. COSATI CODES			18. SUBJECT TERMS (Continue on reverse if necessary and identify by block number)
FIELD	GROUP	SUB-GROUP	
			Fluctuation analysis; liquid/liquid interface; electrochemistry.

19. ABSTRACT (Continue on reverse if necessary and identify by block number)

Voltage fluctuations resulting from transfer of ions at liquid/liquid and gel/liquid interfaces were analyzed. For frequencies higher than the range 6-60 Hz the power spectra were not influenced by the presence of picrate ions in the solution to any major extent. In this range, the resistivity was found to be approximately proportional to the inverse frequency square, both in the absence and in the presence of picrate. By using an equivalent circuit approach, the effect of the cell geometry on the resulting power spectra has been examined.

20. DISTRIBUTION/AVAILABILITY OF ABSTRACT	21. ABSTRACT SECURITY CLASSIFICATION
☒ UNCLASSIFIED/UNLIMITED ☐ SAME AS RPT. ☐ DTIC USERS	unclassified

22a NAME OF RESPONSIBLE INDIVIDUAL	22b. TELEPHONE (Include Area Code)	22c. OFFICE SYMBOL
Jiri Janata	(801) 581-3837	

DD FORM 1473, 84 MAR — 83 APR edition may be used until exhausted. All other editions are obsolete.

SECURITY CLASSIFICATION OF THIS PAGE

ABSTRACT

Voltage fluctuations resulting from transfer of ions at liquid/liquid and gel/liquid interfaces were analyzed. Water/nitrobenzene, Agar gel/nitrobenzene and water/PVC gel-nitrobenzene interfaces were investigated both in the absence and in the presence of picrate ions, dissolved in both phases. For frequencies higher than the range 6 - 60 Hz the power spectra were not influenced by the presence of picrate ions in the solution to any major extent. At lower frequencies, the real component of the equivalent impedance increased significantly less in presence of picrate than in its absence. In this range, the resistivity was found to be approximately proportional to the inverse frequency square, both in the absence and in the presence of picrate. By using an equivalent circuit approach, the effect of the cell geometry on the resulting power spectra has been examined.

INTRODUCTION

In the previous study [1] the thermodynamic data of the transfer of several ions across the poly(vinylchloride)-nitrobenzene gel/water interface were determined by using cyclic voltammetry and zero current potentiometric methods in a four-electrode system. It has been concluded that the difference between the observed equilibrium potential of the transfer of ions at the gel/liquid interface as opposed to the liquid/liquid interface is due to the difference of the diffusion coefficients in the gel-nitrobenzene as opposed to pure nitrobenzene.

In the present study an attempt has been made to characterize these two kinds of interfaces by using fluctuation analysis [2]. The major advantage of this technique, as compared to other small amplitude electrochemical relaxation techniques, lies in the fact that in the fluctuation analysis no perturbation signal is required and thus, the observed system is in the state of true equilibrium during the experiment. The principal disadvantage of the conventional impedance technique applied to the study of the liquid/liquid interfaces is in the change of the interfacial tension, caused by the change of the interfacial potential. This can, in turn, cause a local convection, which may adversely affect the measurement and the evaluation of the parameters of the charge transfer process.

In order to implement the fluctuation analysis for this purpose it is necessary to minimize the area of the interface and maximize the crossection of both the aqueous and of the organic bulk phase. Thus, the power spectrum resulting from the real part of the impedance of the interface can be enhanced and the fluctuations contributed from the

solution resistance can be minimized. The mean amplitude of the fluctuations, $U_n(f)$, is related to the real part of impedance, $Z_{Re}(f)$, by the formula

$$Z_{Re}(f) = U_n(f)^2/4kT\ \Delta f \qquad (1)$$

where f is frequency, and Δf is bandwidth of the spectrum analyzer at frequency f. In order to examine the applicability of the fluctuation analysis to the study of liquid/liquid interface the water/nitrobenzene system with picrate ion was chosen, so that a comparison with the recently published data [3,4] could be done.

EXPERIMENTAL

Chemicals and Cells

Analytical grade lithium chloride (Matheson), tetrabutylammonium chloride (TBACl) and tetrabutylammonium tetraphenylborate (TBATPB) (Aldrich), nitrobenzene (NB) (Fisher), Agar-Agar (Bio-Rad) and poly(vinylchloride) powder (PVC) (Fluka) were used. Sodium picrate (NaPi) was prepared by neutralization of picric acid (Aldrich) with sodium hydroxide, and tetrabutylammonium picrate (TBAPi) by precipitation from equimolar aqueous solutions of TBACl and picric acid. The product was washed by water an recrystallized from acetone. The 3% Agar-gel was prepared in usual way, while the preparation of the PVC gel was described earlier [1].

Three types of galvanic cells were used in this study:

Cell I (Agar gel || nitrobenzene):

Ag/AgCl	0.01 M LiCl 5.10^{-4} M NaPi water	0.01 M LiCl 5.10^{-4} M NaPi 3 % Agar, water	0.01 M TBATPB 5.10^{-4} M TBAPi NB	0.01 M TBACl water'	Ag/AgCl

Cell II (water || nitrobenzene):

Ag/AgCl	0.01 M LiCl 5.10^{-4} M NaPi water	0.01 M LiCl 5.10^{-4} M NaPi 3 % Agar,water	0.01 M LiCl 5.10^{-4} M NaPi water	0.01 M TBATPB 5.10^{-4} M TBAPi NB	0.01 M TBACl water'	Ag/AgCl

Cell III (water || PVC gel-nitrobenzene):

Ag/AgCl	0.01 M LiCl 5.10^{-4} M NaPi water	0.01 M TBATPB 5.10^{-4} TBAPi 20% PVC-NB	0.01 M TBACl water'	Ag/AgCl

The schematic diagrams of these cells are shown in Fig.1. The reason for using the Agar gel in Cell II was to stabilize the position of the water/organic phase interface inside the glass capillary. The gel in the upper compartment acted as a stopper. The excess of the liquid phase at the tip was carefully blotted off with a tissue paper prior to inserting it into the NB phase. The curvature of the meniscus was not taken into account. The cros-sectional area of the solution bulks as well as the surface area of the reference electrodes and reference

interfaces (as the NB/water' interfaces) were by orders of magnitude larger as compared with that of the working interface.

Apparatus and Fluctuation Analysis

The schematic diagram of the equipment used for fluctuation analysis is shown in Fig.2. The impedance transformer was home made from the high input impedance operational amplifier (Analog Devices OPA128) . It was located as close to the investigated cell as possible (about 2 cm), so that the connecting wires between the reference electrodes and the amplifier picked up only a minimum amount of parasitic noise. Both the cell and the amplifier were shielded by heavy brass and stainless steel shielding, to exclude both the electric and magnetic components of electromagnetic noise. The amplifier and the cell were separated from each other by the same multiple shielding (steel/brass/steel), in order to avoid positive feedback or any crosstalk. The output of the impedance transformer was monitored during experiments with a digital voltmeter, to check the DC stability and the potential at the interface. The input of the preamplifier with a bandwidth of 0.03-100,000 Hz was AC-coupled.

A DC analog input coupling, and a flat top window filter for the fast Fourier transform were used with the spectrum analyzer (HP 3582A). The fluctuation analysis experiments were controlled, and all evaluations were done by an HP-86B computer, connected on-line to the spectrum analyzer. Each experiment was performed in the following subsequent frequency spans: 0-25 kHz, 0-2.5 kHz, 0-250 Hz and 0-25

Hz. In each span eight subsequent power spectra were averaged and evaluated. Finally, the average of 2-3 such sets were used to characterize a cell.

Because a logarithmic frequency axis in the impedance plots was needed the raw data points, spaced linearly in each span, were condensed by the computer in such a way that nearly equidistant final points on a logarithmic scale were obtained. To accomplish this a version of the so called third octave analysis [5] was implemented that provided an effective bandwidth of $(2^{1/3}-1)\ f_i$ and an exponential distribution of final frequencies according to formula: $f_{i+1} = 2^{1/3}\ f_i$ where f_i is the frequency of the i-th condensed data point. This algorithm provided an exponentially decaying weighting factor for any set of raw data points, condensed to one final point [6]. This weighting ensured that each final filter was nearly rectangular and symmetrical around the corresponding final frequency on a logarithmic scale and that the relative bandwidths, $\Delta f_i/f_i$, were nearly constant within the whole frequency range involved in this study (0.1-20,000 Hz). Thus, abrupt step changes in the bandwidth at the span boundaries that are characteristic for any digital spectrum analyzer were eliminated.

The equipment and procedure were regularly checked by replacing the cells with standard resistors. The increase of the measured real impedance at low frequencies during these checks was never larger than about 1 % of the increase at the same frequencies when measuring the real cell.

RESULTS AND DISCUSSION

The power spectra, derived from the spontaneous voltage fluctuations at the interfaces, were transformed to real impedance vs. frequency plots according to eq 1 (Fig.3). In order to interpret these results the specific double layer capacitance obtained in previous studies [4,7] was used.

The experiments were performed at a DC potential of about 320 mV this being the potential difference between the bulks of the aqueous and organic phases related to the formal potential difference for the TBA cation transfer [1]. In the previous study [4] when the area of the liquid/liquid interface was 0.192 cm^2, a charge transfer resistance, R_{ct}^P of about 35 Ω and Warburg coefficient, σ^P = 940Ω$s^{-1/2}$ were obtained for the transfer of picrate ion at this potential, using the AC impedance technique with a four-electrode arrangement (see Fig.7 in [4] or similar data in [3]). Value of 10.6 μF cm^{-2} was used for the specific double layer capacity (Table I in [7]). Taking into the account the small surface area of the interface in our experiments (about 1.77×10^{-4} cm^2 in the case of the glass cell, Fig.1A,B), and also the fact that the picrate concentration was half of that used in [4] the actual values used in this study are: $R_{ct}^P \approx 75.9$ kΩ, $C_d \approx 1.87$ nF and $\sigma^P \approx$ 2.04 MΩ $s^{-1/2}$.

At 320 mV, the system is close to the formal potential of the picrate ion transfer (phase equilibrium for picrate). Under the circumstances of the experiments, the charge transfer resistance of the base electrolyte is approximately 20 times higher than that of the picrate ion [4]. Thus, in the presence of picrate, the contribution of the

base electrolyte (characterized by R_{ct}^{b} and σ^{b}) to the cell impedance can be neglected (except for the solution bulks).

Fluctuations originating at all three interfaces contribute to the overall power spectra corresponding to constant resistivities at frequencies above 6-60Hz (Fig.3). In the cell containing PVC-nitrobenzene gel (Fig.3C) the region of constant Z_{Re} is followed by a decay of the real component of impedance at the higher frequencies .

It is plausible to assume that the section of constant Z_{Re} in the range 10 - 10,000 Hz corresponds in each case to the resultant resistance of the solution bulks (and of the gel, if present). This interpretation is supported first of all by the numerical values of the measured impedances, being several hundred kΩ at the Agar gel/liquid and liquid/liquid interfaces, and by one order of magnitude larger at the liquid/PVC gel interface. The decrease of the constant value as caused by the five times increase in the concentration of the background electrolytes (Fig.3A, bottom curve) is also understandable on the basis of this interpretation.

The decay observed at high frequencies in the case of a PVC gel can be understood [8] by realizing that the cut-off frequency, f^{o}_{S}, is significantly depressed with respect to the two other cells by the relatively high specific resistance of the PVC matrix alone:

$$f^{o}_{S} = 1/2\pi R_S C_S \qquad (2)$$

where R_S and C_S are the resulting resistance and capacitance of the equivalent parallel RC of the cell without the interface (see Fig.4A).

The steep low frequency sections must be attributed to processes at the interface because it is the only part of the cell where the presence (absence) of picrate has any significant effect on the measured resistivity. The absolute values of Z_{Re} in this range are significantly smaller in the presence of picrate (Table I). The differences in the slope, **m**, imply that the mechanism of the process in question may be also slightly different depending on the type of interface and on whether only the base electrolyte or also the picrate ion is present.

If the process causing the low frequency decay is modelled, in an approximate manner as a parallel RC network an equivalent circuit of the entire cell can be obtained (see Fig.4A, where the part involving the charge transfer is given in Fig. 5 in Reference 4). The real component of impedance of this circuit in the presence of picrate depends on the circular frequency, ω, as follows:

$$Z_{Re} = \frac{R_S}{1 + (R_S C_S \omega)^2} + \frac{R_I}{1 + (R_I C_I \omega)^2} + \frac{R_{ct} + \sigma \omega^{-1/2}}{1 + 2\sigma C'_d \omega^{1/2} + 2\sigma^2 C'^2_d \omega + 2 R_{ct} C'^2_d \omega^{3/2} + (R_{ct} C'_d \omega)^2} \qquad (3)$$

where the first term describes the impedance of the entire cell except the interface, the second with R_I and C_I corresponds to the low frequency decay and the third describes the charge transfer processes including the Warburg impedance. The upper index p for picrate is

omitted in the second and third term, and C'_d is the combination of the capacitance of the inner layer, C_i, and of the double layer, C_d. As it can be seen, the slope of the low frequency decay in a log-log representation is approximately -2 when $f > f^o_l$.

When only the base electrolyte is present the fluctuation generating components are $R_{ct} = R_{ct}^b$, $\sigma = \sigma^b$ and $R_l = R_l^b$. In the presence of picrate ions, due to the $R_{ct}^P << R_{ct}^b$ and $R_l^P << R_l^b$ conditions, the parallel paths of the base electrolyte in the equivalent circuit can be neglected. The experimental power spectra were compared with those calculated from Eq. 3 using rounded experimental values, i.e. R_{ct}^P = 80 kΩ, C'_d = 2 nF and σ^P =2 M Ω $s^{-1/2}$, respectively (Fig.5). Curve 1 corresponds to the situation when the second term in Eq. 3 is neglected (with R_S = 400 kΩ and C_S = 2 pF). It is obvious from this curve that the Warburg impedance cannot account for the observed low frequency behavior. If we include also the second term (with R_l = 50 GΩ and C_l = 1 nF), the simulated curve becomes similar to the experimental ones (compare curve 2 with the experimental curves in Figs.3A,B). Because of the similar geometrical dimensions the value of C_l was chosen close to C'_d.

In order to simulate the case of the PVC gel a 10 times larger bulk resistance and twice as large resultant capacitance was taken (due to somewhat larger tip diameters and shorter distances). Curve 3 shows the shift of the cut-off frequency of the resultant solution RC impedance into the frequency range of our study, which agrees well with the experimental curves shown in Fig.3C.

The second term of Eq. 3, describing the charge transfer processes at the interface, does not have any significant weight within the range

higher than about 30 Hz. In fact, the changes in the Warburg impedances are small above 500 Hz with respect to the charge transfer resistance (Table II). In that case the parallel circuit in the middle of Fig.4A can be approximated with a simple parallel RC. This justifies the estimate of the cut-off frequency of the charge transfer at 995 Hz (corresponding to the rounded parameters used for simulation, see the arrow in Fig.5). Thus, the charge transfer resistance is hidden in the whole range by the large solution resistances. The Warburg impedance could be resolved only at very low frequencies from the large background signal (see Curve 1). However, the higher value of the slope indicates that it is being covered by fluctuations originating from another process, which is simulated here as a low frequency parallel RC (Curve 2). In the frequency range corresponding to the "knee" on the power spectrum the third term in Eq. 3 dominates the impedance.

If the same concentrations were used, the cut-off frequencies could not be affected by any change in the geometry because they are material constants. However, the simulation shows that certain improvement of resolution of the signal derived from the charge transfer might be possible by using an even smaller interface area, and smaller distances in the solution bulks. Curve 4 was obtained for a 5 times smaller interface diameter, and a net solution resistance of only 50 kΩ, meaning shorter contact paths. A larger value (4 pF) was used for the solution capacitance C_s because of the assumed smaller distances of the reference electrodes. In such a case an abrupt change can be observed around the corresponding cut-off frequency (see the arrow in Fig.5). A flat plateau at low frequencies, however, cannot be obtained even under these anticipated conditions (due to the

contribution of the Warburg impedance) and so the parameters of the charge transfer could be determined only by fitting Eq. 3 to the experimental points. It should be noted that the planar geometry of diffusion at such small interfaces (30 μm diameter) would no longer be completely valid and the radial Warburg impedance [9] would have to be used in the derivation of Eq 3. Thus, by using modified cell and interface dimensions, a resolution of charge transfer processes from cell background could be achieved, at least in principle.

A definitive interpretation of the steep decays of Z_{Re} observed in all cells at low frequencies cannot be made on the basis of these measurements alone. The kinetic parameters characterizing the charge transfer of picrate ions obtained in the previous studies indicate a cut-off frequency of the parallel RC equivalent circuit corresponding to the charge transfer of picrate ion as f^0_{ct} ~ 1120 Hz. Thus, below 1000 Hz only a nearly constant section can be expected to originate from the charge transfer processes of picrate.

It must be mentioned here that an equation for charge transfer, analogous to Eq. 2, defines the cut-off frequency only when the diffusional impedances are absent in the overall ion transfer. In general the cut-off frequency is defined for a parallel RC as $1=(RC\omega)^2$. By the same token for the process involving charge transfer and Warburg impedance the cut-off frequency can be defined from Eq. 3 as

$$1 = 2\sigma C'_d \omega^{1/2} + 2\sigma^2 C'^2_d \omega + 2 R_{ct} C'^2_d \omega^{3/2} + R^2_{ct} C'^2_d \omega^2 \quad (4)$$

Clearly, even under those conditions the flat portion of the spectrum would have a small negative slope due to the $\sigma\omega^{-1/2}$ (Warburg term) in the numerator of the third term in Eq. 3.

In [4], the narrow range of 1-32 Hz was used to determine the charge transfer resistance and Warburg coefficient of picrate ion transfer from AC impedances. When a similarly narrow frequency range,1.6-32 Hz (c.f. arrows in Fig. 3B), was used to evaluate the power spectra in this work a slope of -0.53 was obtained in the log-log representation of the results in Fig.3B. This indicates that for the picrate ion, in this narrow frequency range, Warburg impedance prevails also in our measurements as is also indicated by the simulation (Fig.5, Curve 2). Moreover the value of the Warburg coefficient obtained from the $Z_{Re} - \omega^{-1/2}$ plot in the range 3.2-32 Hz was $\sigma^P = 2.21\ M\Omega\ s^{-1/2}$ in close agreement with $\sigma^P = 2.04\ M\Omega\ s^{-1/2}$ obtained from the AC impedance measurements [4]. The charge transfer resistance, however, could not be determined by the same regression procedure, due to the larger scatter in the spectrum points in fluctuation analysis.

Nevertheless, the part of the spectrum extended to the lower frequency region cannot be interpreted on the basis of diffusional impedances alone because the slope of a power spectrum originating from the Warburg process, cannot be larger than -1/2 in a log-log representation. This is true for a semiinfinite planar diffusion such as would apply to the dimensions of the interfaces used in this study. In other words the effect of the radial diffusion on the Warburg impedance [9] is not expected to be significant for 150 μm diameter area. The experimentally found slopes of the steep curve sections are

around -2 (Table I) which is typical of a Lorentzian spectrum originating from e.g. a parallel RC. The experimental verification of the existence of a process which could be modelled with a parallel RC would require measurements at very low frequencies which are outside the range achievable with our apparatus (despite the fact that our measurements reached frequencies lower by about a decade than those of other measurements [3,4]).

The time constant, τ_l , of the process at the lowest frequencies is relatively large: according to our results, its cut-off frequency is certainly smaller than 0.1 Hz, i.e. τ_l must be larger than 1.6 s. The coupled resistance is also large, in one case even larger than 10^{11} Ω. Consequently, some other interfacial processes must be responsible for the increase of resistivity at low frequencies.

Slow periodic oscillations (f = 0.8 Hz) of current at a similar interface have been observed by Homolka [10]. They could be interpreted as due to slow periodic changes of the surface area of the interface. However, the process responsible for the decay of Z_{Re} in our case can be characterized by a well defined $1/f^2$ noise over a broad frequency band. Another significant difference is that there is no current passing through our interface. Thus, the fluctuations related to some slow but random geometrical changes of the interface could possibly explain this behavior but the cause of such changes may be even harder to rationalize. Another possibility would be a slow adsorption-desorption equilibrium or even precipitation of one salt at the interface as observed by Buck et. al. [11] for chronopotentiometric experiments with tetraalkylammonium iodides. Although the slow adsorption/desorption equilibrium cannot be ruled out the precipitation is not possible under

our conditions because there was no net current passing through the interface which would cause an accumulation in excess of the solubility product and the concentration of picrate was approximately half that of used in the previous work [3,4].

A possible interpretation of the low frequency section, which is no more then a speculation at this point, is the existence of a slow exchange of the solvation shell of the picrate ion. Obviously, all ions transfering from one solvent to another must exchange their solvation shell. This may be a slow process with a high activation energy barrier especially in the case of organic ions which are much larger than typical inorganic ones. Such slow solvation exchange has been observed for the system dimethylacetamide/water [12] but, to our knowledge, no data exists in the literature for the nitrobenzene/water/picrate combination.

The tentative model which would explain the observed behavior therefore consists of the following processes: 1. conduction in organic bulk solution, 2. diffusion between the bulk and interface in the organic diffuse layer, 3. desolvation/solvation equilibrium at the organic boundary of the inner layer, 4. rapid charge transfer of desolvated ions through the inner layer, 5. hydration/dehydration equilibrium at the aqueous boundary of the inner layer, 6. diffusion between that boundary and the aqueous bulk, 7. conduction in the aqueous bulk.

The fine structure of the interface then could be: organic boundary where the desolvation/solvation takes place, inner layer where the charge transfer happens, and the aqueous boundary where the hydration/dehydration happens.

A tentative equivalent electrical circuit corresponding to this model can be proposed (Fig. 4). The possible physical meaning of C_l in the solvation/desolvation RC model could be seen as the change of the microscopic dielectric constant due to the solvent exchange which can be interpeted as an apparent charge partitioning. This C_l corresponds to two capacitors of the area of the interface, of a small (sub-ionic) geometrical thickness; Therefore it may be of the same order of magnitude as that of the inner layer. Such C_l was assumed in the simulations.

The formula for this model is :

$$Z_{Re} = \frac{R_S}{1 + (R_S C_S \omega)^2} + \frac{R_l}{1 + (R_l C_l \omega)^2} + \frac{R_{ct}}{1 + (R_{ct} C_i \omega)^2} + \frac{\sigma}{\omega^{1/2} + 2\,\sigma C_d\,\omega + \sigma^2 C_d^2\,\omega^{3/2}} \qquad (5)$$

where C_d is the double layer capacitance and C_i is the capacitance of the inner layer.

For the sake of simplicity, all symmetrical processes, e.g. for organic and aqueous diffusion, solvation/desolvation (or adsorption/desorption) and for bulk conduction are lumped together, and the upper index p for picrate in terms 2-4 has been omitted. This

model, for the same set of parameters yields similar curves to those obtained by modelling Eq. 3. Its advantage is that it treats the impedance of the inner layer (charge transfer impedance) and the impedance of the diffuse layer, separately. Also, in the case of multiple ion transfer the individual charge transfer processes are parallelly coupled that can be explicitely taken into account in Eq 5. Such representation is closer to reality than that shown in Fig. 4A.

CONCLUSIONS

The random voltage fluctuations can be used to characterize the electrochemical processes which occur at the immiscible liquid/liquid interfaces. This approach is complementary to the traditional impedance technique. In fact it is its limiting case when the amplitude of the excitation signal tends to zero. For this reason it is capable of furnishing information about the interface in the state of equilibrium. The principal limitation of the fluctuation analysis is that it yields information only about the real component of the impedance spectrum. In order to resolve the individual components of the Z_{Re} it is necessary to analyze the power spectrum over a wide range of frequencies.

In order to access the low frequencies for the fluctuation analysis of the liquid/liquid interface it is necessary to optimize the cell geometry and the concentrations. Small surface area of the interface is required in order to obtain intensive signals. However, the radial form of diffusion must be considered for diameters smaller than 10 μm. The signal-to-noise ratio should be enhanced by the short distances between the interface and the reference electrodes. It is not possible

to use a 3 or 4 electrode arrangement, because any additional contact would act as a shunt, and short out the voltage fluctuations. Therefore, at equilibrium the interfacial potential is set up and maintained only by chemical means i.e. by the proper activities of the primary ions and of the background electrolytes. It is described by the equation derived by Buck and Melroy (Eq. 6 in Ref. 13), which represents an equilibrium analog of the Nikolskij-Eisenman equation.

Because the frequency range of the fluctuation analysis is lower than that reported for conventional impedance measurements in the field of ITIES, the contribution of the Warburg noise is more visible in this study. Nevertheless, the low frequency part of our results, cannot be interpreted on the basis of Warburg impedance alone.

The possible importance of the slow solvation/hydration processes preceding and following the charge transfer is plausible. As a consequence, a more detailed model of the interfaces studied in this work can be suggested which includes such processes.

REFERENCES

1 V. Marecek, M.P. Colombini, *J. Electroanal. Chem.*, **241** (1988) 133

2 A.Bezegh and J.Janata, Anal.Chem., 59 (1987) 494A

3 T. Osakai, T. Kakutani, M. Senda, *Bull. Chem. Soc. Japan*, **58** (1985) 2626

4 T. Wandlowski, V. Marecek, Z. Samec, *J. Electroanal. Chem.*, **242** (1988) 291

5 ANSI Spec. S1.11-1966, *American National Standard Specification for Octave, Half-Octave and Third-Octave Band Filter Sets,* ANSI, Inc., 1430 Broadway, New York, NY 10018 (1966)

6 M. Gratzl, J.Janata, J.Phys.E, submitted (1989)

7 Z. Samec, V. Marecek, D. Homolka, *J. Electroanal. Chem.*, **158** (1983) 25

8 Z.Samec, Chem.Rev., 88 (1988) 617

9 A.Bezegh, J.Janata, *J. Electroanal. Chem.*, **215** (1986) 139

10 D.Homolka, V.Marecek, *J. Electroanal. Chem.*, **112** (1980) 91

11 W.E.Bronner, O.R.Melroy and R.P.Buck, J.Electroanal.Chem., 162 (1984) 263

12. J.Janata and R.D. Holtby-Brown, JCS Perkin II, (1973) 991

13. O.R.Melroy and R.P.Buck, J.Electroanal.Chem. 143 (1983) 23

ACKNOWLEDGEMENT

This work was supported by the contract from the Office of Naval Research

Table I.

Results of Linear Regression for the Low Frequency Decay in log-log Representation

interface	base el. M	picrate M	$lg(Z_{Re}) = m\ lg(f) + c$		$Z_{Re} = C\ \omega^m$
			m	c	C ($\Omega\ s^{-m}$)
Agar/NB	0.01	-	-1.9	7.9	2.6×10^9
(Cell I)	0.01	0.0005	-1.6	7.4	4.8×10^8
	0.05	0.0005	-2.0	6.8	2.5×10^8
water/NB	0.01	-	-1.6	7.9	1.5×10^9
(Cell II)	0.01	0.0005	-2.1	6.7	2.4×10^8
water/PVC	0.01	-	-3.4	8.0	5.2×10^{10}
(cell III)	0.01	0.0005	-1.5	7.2	2.5×10^8

Table II.

Weight of the Picrate Charge Transfer Resistance and the Warburg Impedance at Different Frequencies[x]

f (Hz)	3	30	115[e]	300	1120[o]	3000
$Z_{w,Re} = \sigma\omega^{-1/2}$ (kΩ)	470	149	75.9	47.0	24.3	14.9

[x] the experimental values for picrate transfer [4] are used (R_{ct}=75.9 kΩ, C'_d = 1.07 nF and σ=2.04 MΩ $s^{-1/2}$), and the real part of the diffusional impedance is calculated; its absolute values can be obtained by multiplying the numbers in the Table by √2

[e] frequency at which the real Warburg impedance equals the charge transfer resistance

[o] cut-off frequency of the parallel RC of charge transfer, when the diffusional impedance is neglected (the approximate cut-off)

LEGENDS TO THE FIGURES

Fig.1 Construction of the cells

A) Agar gel/nitrobenzene interface (Cell I, gel/liquid)

B) Water/nitrobenzene interface (Cell II, liquid/liquid)

C) Water/PVC gel-nitrobenzene interface (Cell III, liquid/gel)

1 Ag|AgCl reference electrode

2 aqueous phase (w')

3 aqueous phase (w)

4 cut polypropylene pipet tip

5 organic phase (o)

6 Teflon capillary, i.d. 0.3 mm, o.d. 1.5 mm

7 PVC-nitrobenzene gel

8 glass capillary, tip i.d. 150 μm

9 Agar gel

Fig.2 Apparatus for fluctuation analysis

solid line: brass wall

dashed line: stainless steel wall

thin arrows: analogue signal

thick arrows: digital signal

R_1 and R_2: Ag/AgCl reference electrodes used as electric contacts to the cell

Fig.3 Experimental results: log-log plots of the real component of impedance as a function of frequency

A) Agar gel/nitrobenzene interface (Cell I, gel/liquid)

B) water/nitrobenzene interface (Cell II, liquid/liquid)

C) water/PVC gel-nitrobenzene (Cell III, liquid/gel)

□ 0.01 M base electrolytes

■ 0.01 M base electrolytes + 5.10^{-4} M picrate ions

◆ 0.05 M base electrolytes + 5.10^{-4} M picrate ions

Straight line: result of linear regression between the log-log variables. The ends of the line indicate the limits of the regression interval.

Fig.4 Approximate equivalent circuits of the cells: (A) with unresolved inner and diffuse double layer, and (B) with the inner and diffuse layers as well as the organic and aqueous phases separated. Dotted line represents the hypothetical element to account for the low frequency section of the power spectra. Shadowed box is the diffusional (Warburg) impedance.

R_S, C_S equivalent resistance and capacitance of the cell except the interface (gel is included if present)

R_{ct},σ,C_d charge transfer resistance, Warburg coefficient and double layer capacitance of the interface

R_l, C_l equivalent resistance and capacitance characterizing the interface process responsible for the observed low frequency decay

C_i capacitance of the inner layer

C_d' combination of C_d and C_i

b,p base electrolyte and picrate ion (as upper indices)

The value of the any parameter is generally different for the organic and aqueous phases and so, for simplicity, identical symbols denote different values if they characterize different phases.

Fig. 5 Simulated resistivity - frequency plots. Calculations were performed with Eq. 3.

1 R_{ct}=80 kΩ, σ=2 MΩ $s^{-1/2}$, C'_d=2 nF, R_S= 0.4 MΩ, C_S=2 pF (the low frequency RC is not involved)

2 as Curve 1, and R_I=50 GΩ, C_I=1 nF

3 R_{ct}=80 kΩ, σ=2 MΩ $s^{-1/2}$, C_d=2 nF, R_S=4 MΩ, C_S=4 pF, R_I=50 GΩ, C_I=1 nF

4 R_{ct}=1 MΩ, σ=50 MΩ $s^{-1/2}$, C_d=80 pF, R_S=50 kΩ, C_S=4 pF, R_I=1250 GΩ, C_I=40 pF

arrow: approximate cut-off frequency of the charge transfer process (995 Hz) at the rounded charge transfer parameters

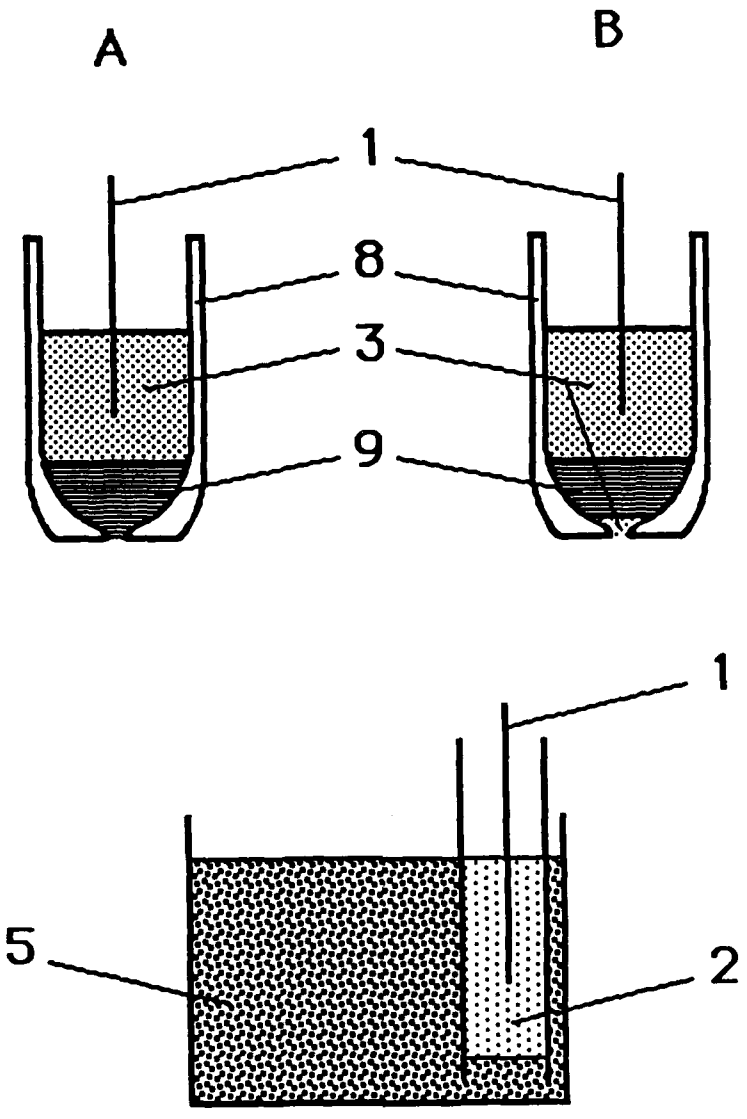

Fig. 1
(A, B)

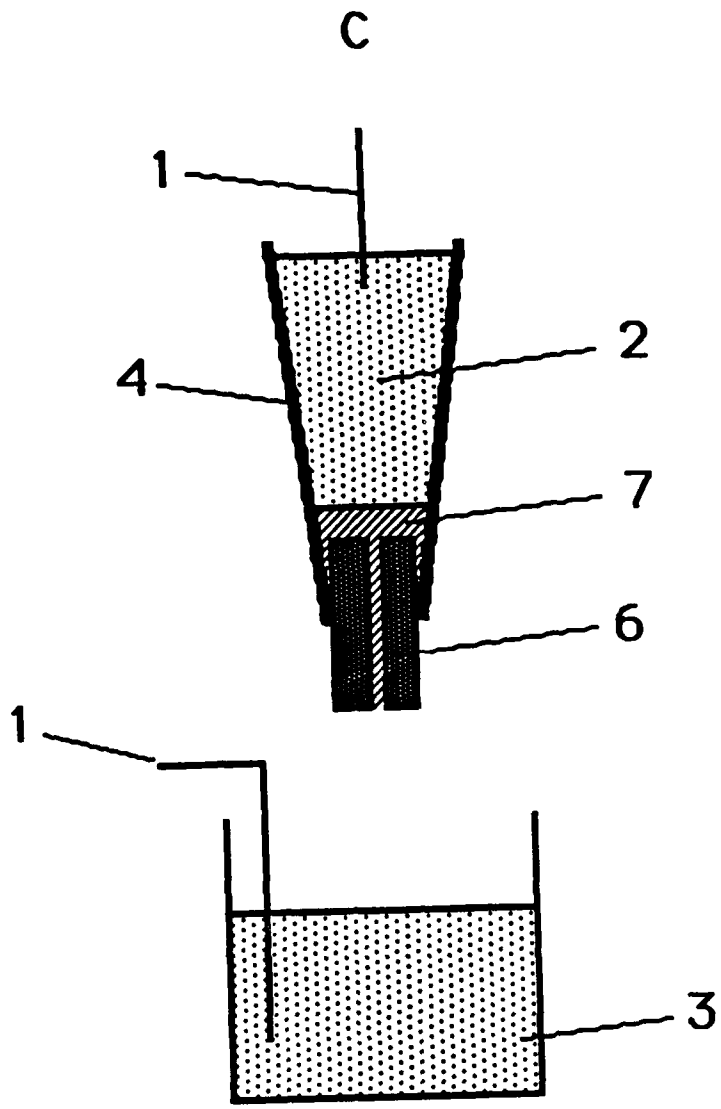

Fig 1.
(C)

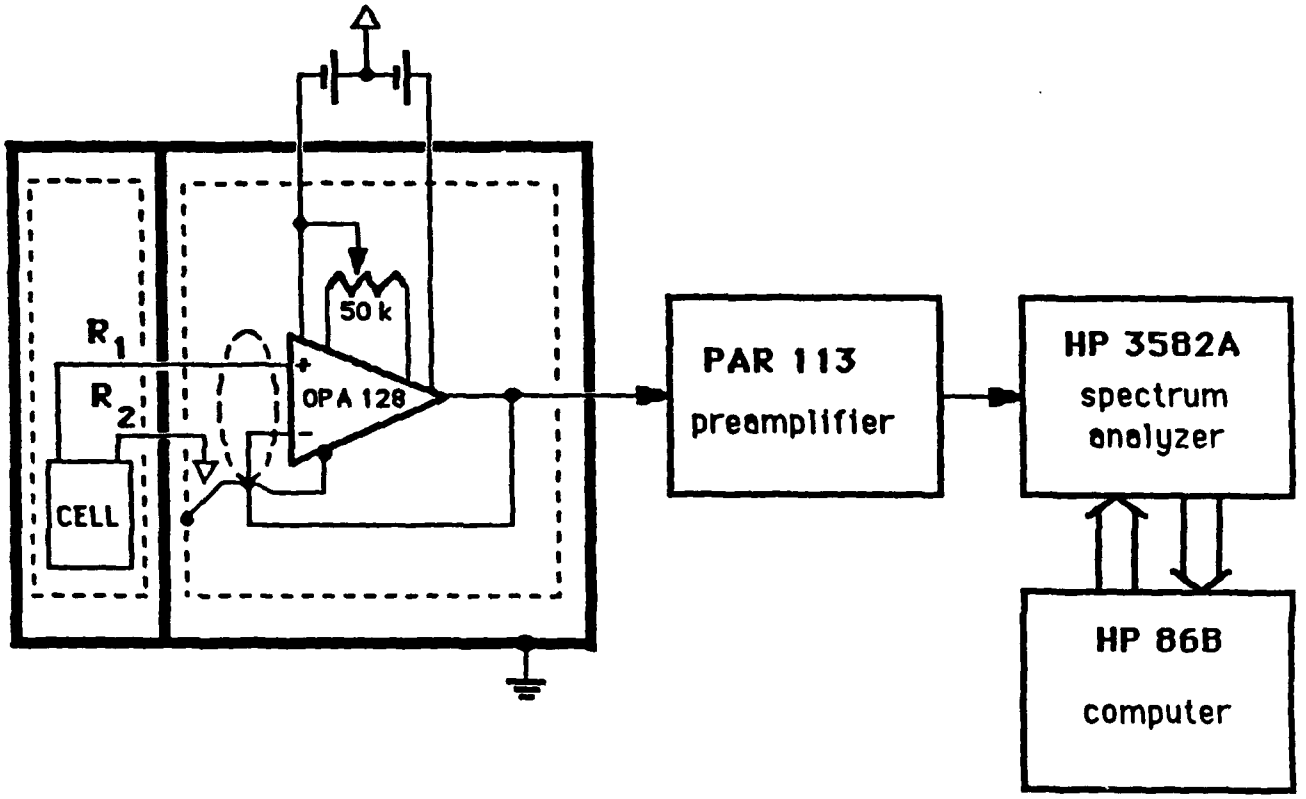
50 k
R1
R2
OPA 128
CELL
PAR 113
preamplifier
HP 3582A
spectrum
analyzer
HP 86B
computer

Fig. 2.

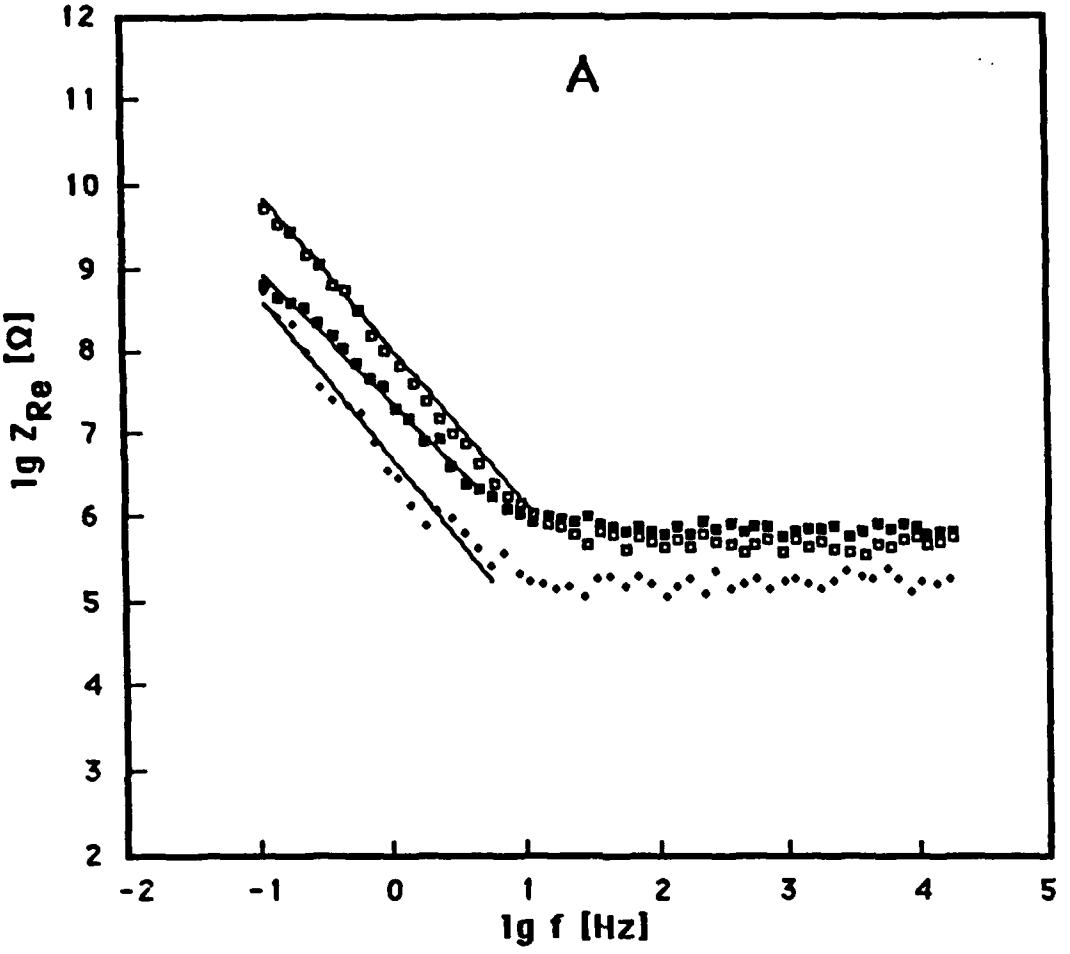

Fig. 3 A.

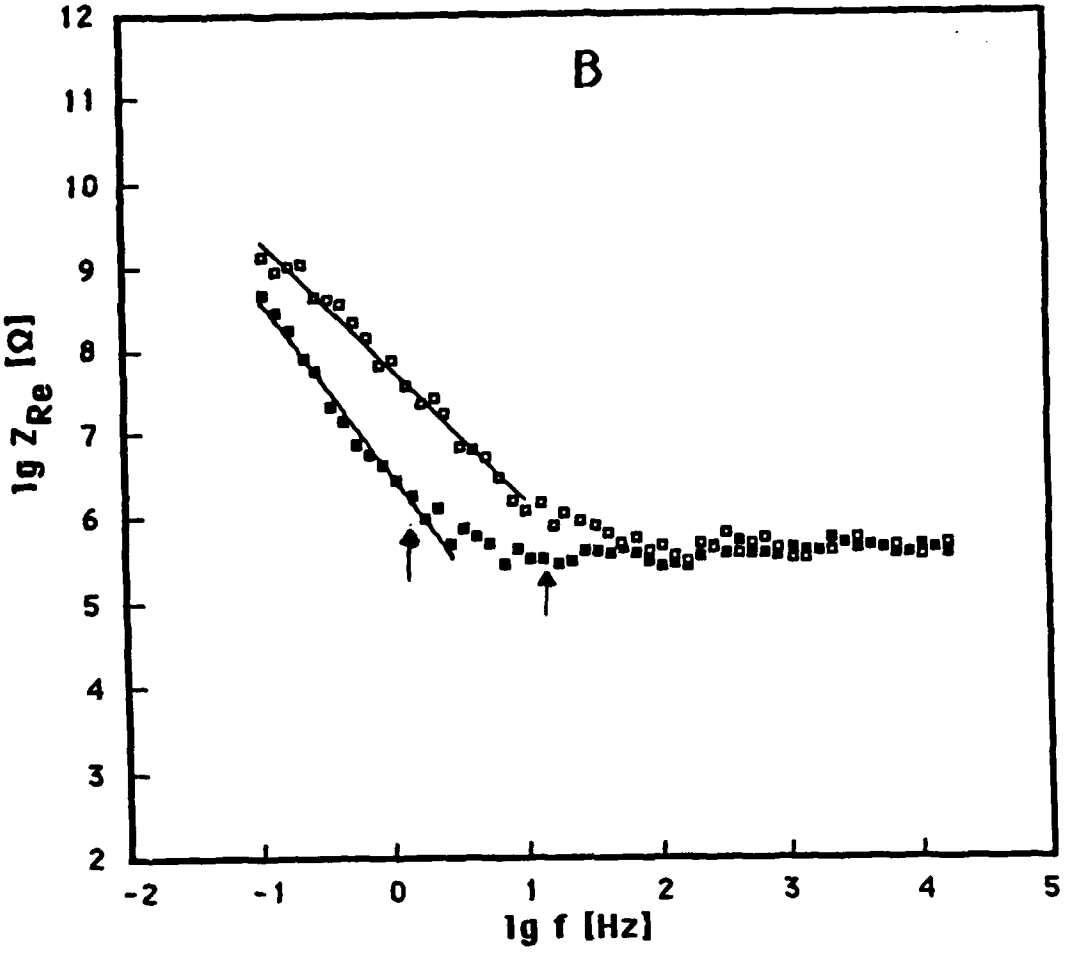

Fig. 2B.

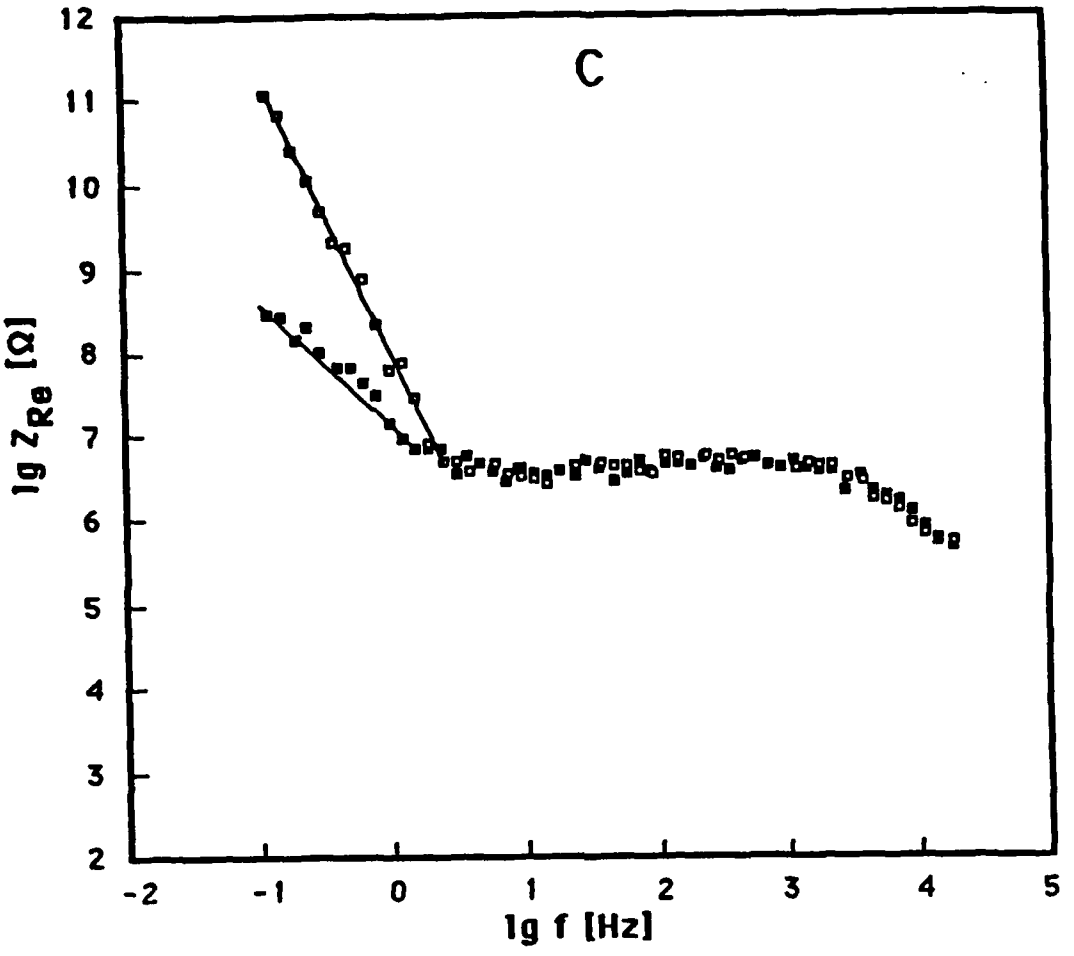

Fig. 2C.

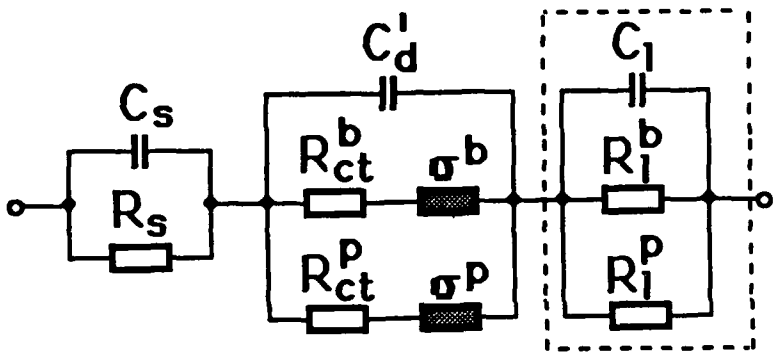

A

Fig. 4A.

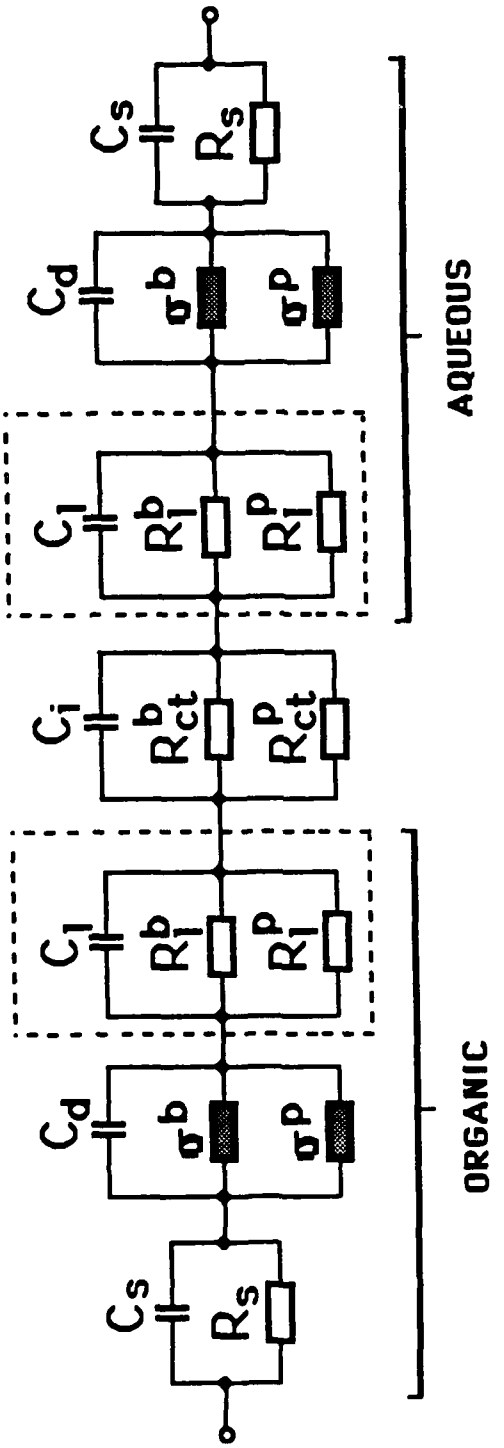
C_s
R_s
C_d
σ^b
σ^p
AQUEOUS
C_i
R_i^b
R_i^p
C_i
R_{ct}^b
R_{ct}^p
C_i
R_i^b
R_i^p
C_d
σ^b
σ^p
ORGANIC
C_s
R_s

B

Fig 4B.

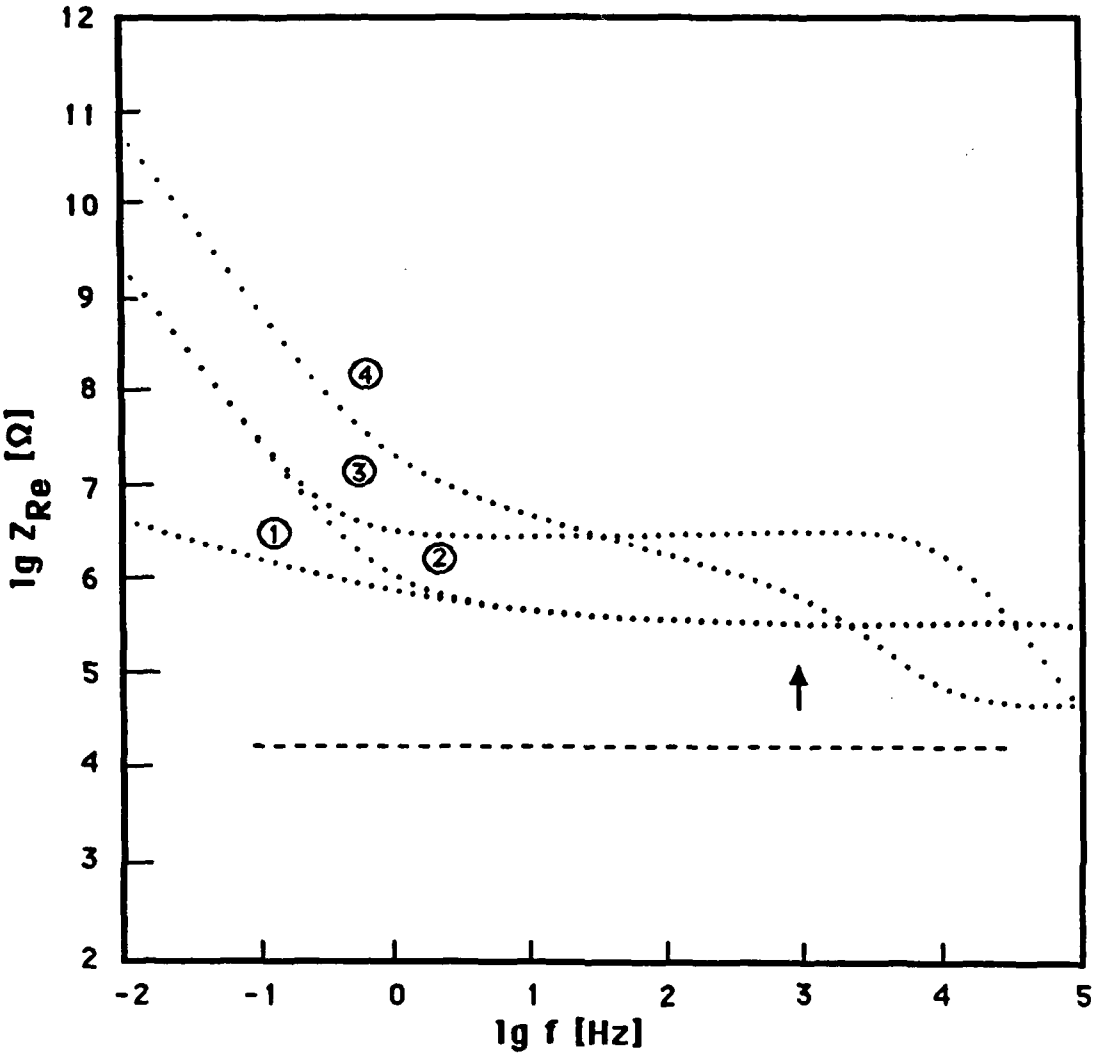

Fig. 5.